DOI: https://doi.org/10.1051/e3sconf/202016800046

CONVERSION OF GAS ENGINE WASTE HEAT INTO COLD USING ABSORPTION CHILLERS

[1]*Georgii Karman*, [2]*Yurii Oksen*, [2]*Olena Trofymova*, [2]*Yurii Komissarov*, [2]*Borys Dizhevskyi*, [2]*Maksym Radiuk*, [3]*Inna Diakun*

[1]*General Electric*, [2]*National Technical University "Dnipro Polytechnic"*, [3]*Institute of Geotechnical Mechanics named by N. Poljakov of National Academy of Sciences of Ukraine*

Abstracts. A possibility of gas engine waste heat conversion into cold for air conditioning in mines using lithium bromide absorption chillers is investigated. Dependencies of parameters of a thermodynamic cycle and energy indicators of chillers on temperatures of a heating medium and a coolant are obtained using mathematical modelling. It is shown that it is rational to use two chillers with sequential movement of a heating medium and a coolant through them in opposite directions for a full conversion of gas engine waste heat. COP of such a system is 0.733. This allows obtaining 2140 kW of cooling capacity with a coolant temperature of 7°C when using a gas engine JMS-620 by Jenbacher.

Introduction. Non-traditional energy-saving technologies [1 – 15] start to be applied more widely in coal mines of Ukraine at the present time. These technologies include heat pumps based on low-potential heat and technologies of burning coal mine methane using gas engines (GE). GEs are cogeneration plants (modules) that generate electrical energy and waste heat for heating systems [1]. In some cases, large amounts of generated waste heat are "dumped" into the environment due to the lack of heat consumers. A possibility of converting this heat into additional electric energy is studied in the papers [13 - 15]. Excess waste heat of GEs can be converted into cold for air conditioning using lithium bromide absorption chillers (LBAC) in deep coal mines that require air conditioning of mine workings. The usage of LBAC instead of the traditionally used vapor-compression refrigeration systems significantly reduces consumption of electric energy and operating costs of generation of cold. There are known cases of generation of cold using LBAC in the world practice of air conditioning in mines, including those when waste heat from GEs is converted into cold [16].

The goal of this research is to determine thermal modes and energy efficiency of LBAC during utilization of GE waste heat and generation of cold for air conditioning in coal mines under the conditions of a specific scheme of LBAC and temperature modes of heating and cooled media.

Methods. GE JMS-620 by Jenbacher is currently used in Ukrainian mines. This module generates 3035 kW of electric energy and 2920 kW of thermal energy in a form of hot water from the engine cooling system. The water temperature varies from 110 to 70 °C as a result of heat loss. Consider a single-stage LBAC as a consumer of heat, the scheme of which is shown in Figure 1.

A refrigerant is water vapor and an absorbent is a water solution of lithium bromide LiBr.

The liquid refrigerant is converted into steam in the evaporator E due to the specific refrigerating capacity q_0 supplied from an external source (coolant of the air conditioning system). The steam enters the absorber A and is absorbed by the water

solution of LiBr. The specific thermal load of absorber q_a is removed by cooling water. A weak solution (with a low concentration of LiBr) is supplied to the generator G by the pump P1 through the heat exchanger of solutions HE.

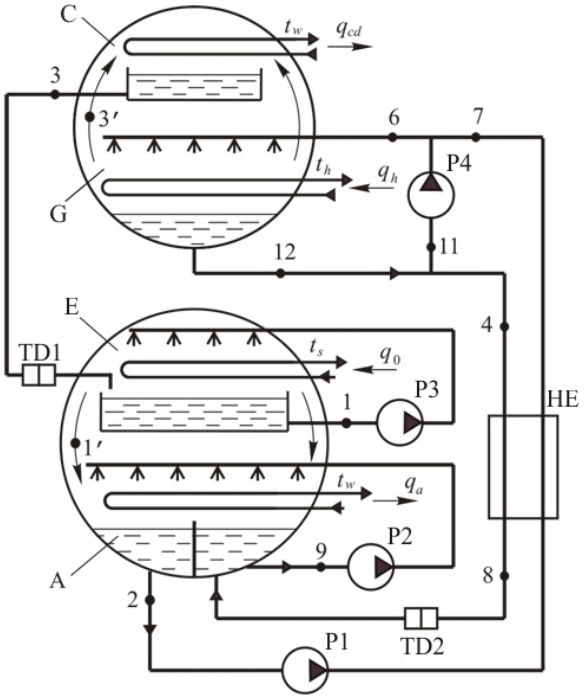

A – absorber, E – evaporator, G – generator, C – condenser, HE – het exchanger of solutions, P1, P2, P3, P4 – pumps, TD1 and TD2 – throttling devices; t_s, t_h, t_w, – temperatures of a coolant, heating and cooling media, °C; q_0, q_{cd}, q_a, q_h – specific refrigerating capacity and specific thermal loads of a condenser, absorber, generator, kJ/kg, the numbers indicate characteristic points of flows of working media

Figure 1 – Scheme of LBAC

The weak solution is heated in the heat exchanger of solutions HE by the heat received from the strong solution (with a high concentration of LiBr), which comes from the generator G. The refrigerant is evaporated from the solution in the generator G due to the specific thermal load q_h obtained from the heating medium (hot water from the GE cooling system) and is directed to the condenser C. Almost pure water vapor is evaporated in the generator G since the boiling points of water and lithium bromide are very different. The refrigerant vapor gives specific thermal load q_{cd} to the cooling water and condenses in the condenser C. The condensate is discharged into the evaporator E through the throttling device TD1. The strong solution of LiBr is discharged into the absorber A through the throttling device TD2 after passing through the heat exchanger of solutions HE.

The absorber A and the evaporator E are located in the lower drum, and the generator G and the condenser C are located in the upper drum. The absorber A and the generator G are film type devices. Their usage allows reducing thermodynamic losses from incomplete solution evaporation during the steam generation and incomplete solution saturation during the absorption compared to the flooded devices. The scheme provides recirculation of solutions and a refrigerant by using pumps P2,

P3 and P4 in order to intensify the heat and mass transfer processes.

The operating process of LBAC is graphically represented in Figure 2 in h, ξ – coordinates (h is enthalpy, kJ/kg, ξ is mass concentration of lithium bromide in a solution, %). The cycle of solution state change 2 - 7 - 6 - 5 - 4 - 8 - 9 - 10 - 2 is shown on the background of isobars p_a and p_h of a saturated liquid. Isobars of the superheated water vapor, which is in equilibrium with the saturated solution of LiBr, are shown in the upper part of the figure. The numbers of characteristic points of the process correspond to the numbers of points shown in the scheme of LBAC (Fig. 1).

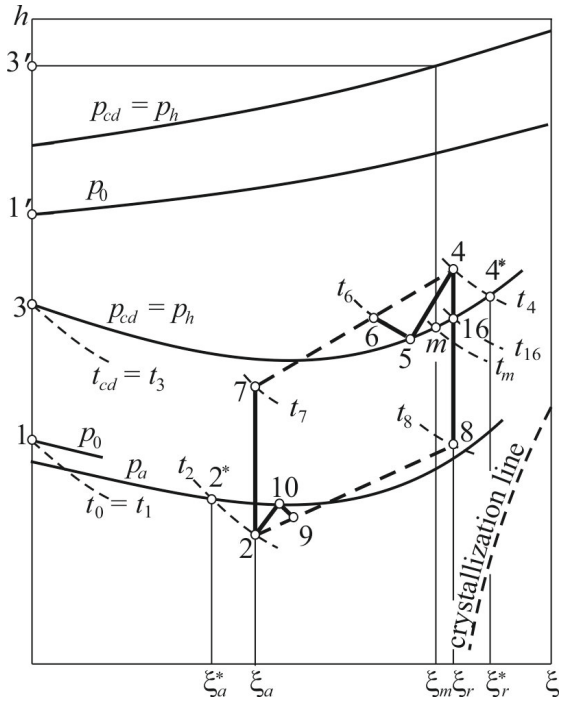

p_h, p_{cd}, p_0, p_a are pressures in generator G, condenser C, evaporator E, and absorber A, respectively, Pa; ξ_a, ξ_r and ξ^*_a, ξ^*_r are concentrations of LiBr in weak and strong solution for real and theoretical cycle, respectively, %; ξ_m is concentration of LiBr in solution with parameters of state at point m, %; $t_1 - t_{16}$, t_m are solution temperatures at characteristic points of process, °C; t_0, t_{cd} are boiling and condensation points, respectively, °C

Figure 2 – Scheme of operating process of LBAC

During the analyzing of operating process assume that:

- pressures in the operating space of the generator G and condenser C blocks are equal

$$p_h = p_{cd}; \tag{1}$$

- pressure p_0 in the evaporator E exceeds pressure p_a in the absorber A by the amount of hydraulic losses

$$\Delta p_a = p_0 - p_a; \tag{2}$$

- concentration of the weak solution at the absorber A outlet (at point 2) ξ_a differs from the equilibrium one ξ^*_a for a temperature t_2 at point 2 by the amount of incompleteness of saturation

$$\Delta\xi_a = \xi_a - \xi_a^*; \quad (3)$$

- concentration of the strong solution at the generator G outlet (at point 4) ξ_r differs from the equilibrium one ξ^*_r for a temperature t_4 at point 4 by the amount of incompleteness of evaporation

$$\Delta\xi_r = \xi_r^* - \xi_r. \quad (4)$$

Lines 2 - 7 and 4 - 8 in Figure 2 correspond to processes of heating the weak and cooling the strong solution in the heat exchanger of solutions HE. Point 6, which determines the state of solution before the generator G nozzles, is located on a line 7 - 4 of mixing of solutions with parameters of states at points 7 and 4. Similarly, point 9 is located on a line 8 - 2 of mixing of solutions with parameters of states at points 8 and 2. The solution is superheated at point 6 compared to a saturation state at temperature t_6 and pressure p_h in the generator G. The solution is supercooled at point 9 compared to a saturation state at temperature t_9 and pressure p_a in the absorber A. Processes 6 - 5 and 9 - 10 are considered isobaric-adiabatic. The refrigerant is evaporated during process 6 - 5 due to reduction of the solution enthalpy. Further evaporation of the refrigerant occurs during process 5 - 4 due to the supply of heat from the heating medium. The solution superheats in this case and the resulting refrigerant vapor is in a state of equilibrium with a saturated solution. The state of saturated solution changes along line 5 - 16. Assume that the temperature of formed refrigerant vapor is equal to the average solution temperature t_m on line 5 – 16

$$t_m = (t_5 + t_{16})/2. \quad (5)$$

The refrigerant vapor state at the generator G outlet (condenser inlet) is determined by point 3′, at the condenser C outlet – by point 3, at the evaporator E outlet – by point 1′ in the scheme. All these points are located on the vertical $\xi = 0$.

The initial data for calculating the parameters and constructing the cycle are:

t_{s2} is final temperature of cooled coolant, °C;

t_{h2} is final temperature of heating medium, °C;

t_w is final temperature of cooling water, °C;

$\Delta t_{2\text{-}8}$ is temperature difference at a cold end of a heat exchanger of solutions HE, °C;

Δt_a, Δt_g, Δt_{ev} and Δt_{cd} are minimum temperature differences in absorber A, generator G, evaporator E and condenser C, °C;

Δp_a are refrigerant vapor pressure losses during movement from evaporator E to absorber A, Pa;

$\Delta\xi_a$ is incompleteness of saturation of solution in absorber A, %;

$\Delta\xi_r$ is incompleteness of evaporation of refrigerant in generator G, %;

α_g is coefficient of recirculation of solution in generator G, which is a ratio of mass flow rates of strong solution m at points 11 and 4 (Fig. 1):

$$\alpha_g = m_{11}/m_4. \quad (6)$$

Calculation of parameters at the characteristic points of the cycle is performed in the following way.

Temperature of the weak t_2 and strong t_4 solutions at the absorber and generator outlet (at points 2 and 4, respectively) is determined. The boiling t_0 and condensation t_{cd} points of the refrigerant at the evaporator E and the condenser C outlet (at points 1 and 3, respectively), and the temperature t_8 of the strong solution at the outlet of heat exchanger of solutions (at point 8) are determined:

$$t_2 = t_w + \Delta t_a, \tag{7}$$

$$t_4 = t_h - \Delta t_g, \tag{8}$$

$$t_0 = t_1 = t_s - \Delta t_{ev}, \tag{9}$$

$$t_{cd} = t_3 = t_w + \Delta t_{cd}, \tag{10}$$

$$t_8 = t_2 + \Delta t_{2-8}. \tag{11}$$

The saturated water vapor pressure in the evaporator E p_0 and in the condenser C p_{cd} are determined using the temperatures t_0 and t_{cd}. The pressure in the generator G p_h and the absorber A p_a. is determined using the formulas (1) and (2).

Concentration of the weak solution ξ_a^* is determined from the pressure p_0 and the temperature t_2, concentration of the strong solution ξ_r^* – from the pressure p_h and the temperature t_4 (for the theoretical cycle – when losses from incomplete saturation of the solution in the absorber A and incomplete evaporation in the generator G are absent). Concentration of the weak ξ_a and strong ξ_r solution for the real cycle is determined using the formulas (3) and (4). After that, the location of points 2, 4, 8 and the solution enthalpy in these points are determined using temperatures and concentrations.

Enthalpy of the heated weak solution (at point 7) is calculated using the heat balance equation of the heat exchanger of solutions HE

$$q_{he} = (f-1)(h_4 - h_8) = f(h_7 - h_2), \tag{12}$$

where q_{he} is heat flow in heat exchanger, kJ/kg; h_4, h_8, h_7, h_2 is solution enthalpy determined at points 4, 8, 7, 2, kJ/kg; f is circulation ratio, determined using formula

$$f = \frac{m_a}{m_v} = \frac{m_7}{m_3} = \frac{\xi_r}{\xi_r - \xi_a} = \frac{\xi_r}{\Delta\xi}, \tag{13}$$

where m_a and m_v are mass flow rates of the weak solution of LiBr entering the generator G and water vapor leaving the generator G, kg/s; $m_3 = m_v$ and $m_7 = m_a$ are mass flow rates of media at points 3 and 7 of the scheme of LBAC, kg/s (Fig. 1).

Parameter $\Delta\xi = \xi_r - \xi_a$ in formula (13) is the solution degassing zone, %. The enthalpy and concentration of LiBr of the resulting flow (at point 6) is calculated using the equations of heat balance and material balance for LiBr salt for the mixing

point of flows with parameters of points 7 and 11:

$$h_6 = \frac{m_{11}h_{11} + m_7 h_7}{m_6} = \frac{\alpha_g (f-1) h_4 + f h_7}{\alpha_g (f-1) + f}, \quad (14)$$

$$\xi_6 = \frac{m_{11}\xi_{11} + m_7 \xi_7}{m_6} = \frac{\alpha_g (f-1) \xi_4 + f \xi_7}{\alpha_g (f-1) + f}, \quad (15)$$

where m_6 and m_{11} are mass flow rates of solution at points 6 and 11 of scheme of LBAC, kg/s; h_{11} is enthalpy of solution at point 11, kJ/kg; ξ_4, ξ_7, ξ_{11} are mass concentrations of LiBr in solution at points 4, 7, 11, %.

Balance equations are characteristic for the isobaric-adiabatic process 6 - 5 of separation of the superheated solution into the saturated solution with parameters of state at point 5 and the superheated water vapor, which is in equilibrium with a saturated solution:

$$m_6 = m_5 + m_{v5}, \quad (16)$$

$$m_6 h_6 = m_5 h_5 + m_{v5} h_{v5}, \quad (17)$$

$$m_6 \xi_6 = m_5 \xi_5, \quad (18)$$

where h_{v5} and m_{v5} are enthalpy of water vapor (kJ/kg) formed in process 6 – 5, and water vapor mass flow rate (kg/s); m_5 is mass flow rate of solution at point 5 of scheme of LBAC, kg/s; h_5 and h_6 are enthalpies of solution at points 5 and 6, kJ/kg; ξ_5 and ξ_6 are mass concentration of LiBr in solution at points 5 and 6, %.

Then the concentration of LiBr, the saturated solution enthalpy at point 5 of the cycle, the parameters of the water vapor, which is in equilibrium with a saturated solution, and the mass flow rates m_5 and m_{v5} are calculated using equations (16) - (18). This is performed considering the dependencies of enthalpy of saturated solution and of superheated water vapor, which is in equilibrium with a saturated solution, depending on the temperature and concentration of LiBr.

The water vapor enthalpy $h_{3'}$, which is formed as a result of the solution boiling during process 5 – 4 is determined using the concentration ξ_m and the pressure p_h. The enthalpy of saturated water vapor $h_{1'}$ at the evaporator E outlet (at point 1′) is determined using the temperature t_0.

Calculation of thermodynamic parameters of the solution of LiBr and water vapor are calculated using the formulas given in papers [17, 18].

Energy characteristics of the cycle are calculated after determining the parameters at the characteristic points of the cycle: specific refrigerating capacity q_0, specific thermal loads of condenser C q_{cd}, absorber A q_a, generator G q_h (kJ/kg) and coefficient of performance (COP):

$$q_0 = h_{1'} - h_3, \quad (19)$$

$$q_{cd} = h_{3'} - h_3, \quad (20)$$

$$q_a = h_{1'} + f(h_8 - h_2) - h_8, \quad (21)$$

$$q_h = h_{3'} + f\left(h_4 - h_7\right) - h_4, \tag{22}$$

$$COP = \frac{q_0}{q_h}. \tag{23}$$

COP indicates how much cold can be obtained in the evaporator E during consumption of a unit of heat in the generator G.

The following limitations are applied to the parameters of cycles of LBACs. The mass concentration ξ_r of the strong solution of LiBr must not exceed 64 % due to the danger of crystallization [19], and the solution degassing zone $\Delta\xi$ should be in a range of 3.5 to 4.5 % [20], according to the rational hydraulic conditions of the absorber A and the generator G.

Results and discussion. The specific refrigerating capacity q_0 produced by LBAC depends on the amount of specific thermal load q_h and the chiller COP as shown in the formula (23). These values depend on external conditions, i.e., on the temperatures of heating medium t_h and the coolant t_s. The temperature t_h of heating medium (water from the GE cooling system) can vary from $t_{h1} = 110$ °C to $t_{h2} = 70$ °C. The coolant of air conditioning systems is cooled in chillers by 10 ... 12 °C [21 - 23]. Therefore, the boundaries of changes of temperature range can be assumed equal to $t_{s1} = 17$ °C and $t_{s2} = 7$ °C.

Calculations are performed according to the method described above in order to establish the influence of temperatures of heating and cooled media on a thermal mode and LBAC efficiency.

The following parameters are assumed for calculations:

- final temperature of the water cooling the condenser C and the absorber A, $t_w = 26$ °C;
- temperature difference at the cold end of the heat exchanger of solutions HE $\Delta t_{2\text{-}8} = 15$ °C;
- minimum temperature difference in the absorber A, generator G, evaporator E and the condenser C, respectively $\Delta t_a = 6$ °C, $\Delta t_g = 5$ °C, $\Delta t_{ev} = 3$ °C and $\Delta t_{cd} = 4$ °C;
- refrigerant vapor pressure losses during movement from the evaporator E to the absorber A $\Delta p_a = 0.13$ kPa;
- incompleteness of saturation of the solution in the absorber A $\Delta\xi_a = 0.5$ %;
- incompleteness of evaporation of the refrigerant in the generator G $\Delta\xi_r = 1.5$ %;
- coefficient of recirculation of the solution in the generator G $\alpha_g = 3.0$.

The main calculation results are given in table 1. Graphs of COP dependencies on final temperatures of heating and cooled medium are built in Fig. 3 and 4.

COP, width of the degassing zone $\Delta\xi$, and the concentration of the strong solution ξ_r increase during increase of temperatures t_h and t_s, as shown in Table 1, Figure 3, and Figure 4. The concentration of the strong solution ξ_r reaches the 64 % boundary value from the condition of solution crystallization at $t_h = 91$ °C (calculation mode 9, Table 1). A decrease of t_h leads to narrowing of the degassing zone, which at 81 °C (mode 3) becomes equal to the lower boundary of the 3.5 ... 4.5 % range recommended in the paper [20].

Table 1 – Calculation results of thermal modes of LBAC

Mode	t_h, °C	t_s, °C	ξ_a, %	ξ_r, %	f	q_h, kJ/kg	q_a, kJ/kg	q_{cd}, kJ/kg	q_0, kJ/kg	η	Δξ, %
1	79.0	7.00	56.22	58.74	23.26	3466.3	3343.1	2505.9	2382.6	0.687	2.526
2	80.0	7.00	56.22	59.20	19.88	3369.7	3244.9	2507.5	2382.6	0.707	2.977
3	81.0	7.00	56.22	59.65	17.39	3300.2	3173.7	2509.1	2382.6	0.722	3.429
4	82.0	7.00	56.22	60.09	15.51	3248.9	3120.8	2510.7	2382.6	0.733	3.875
5	83.0	7.00	56.22	60.53	14.03	3209.8	3080.2	2512.3	2382.6	0.742	4.314
6	84.0	7.00	56.22	60.97	12.83	3179.0	3047.7	2513.9	2382.6	0.750	4.754
7	86.0	7.00	56.22	61.84	11.00	3134.7	3000.3	2517.0	2382.6	0.760	5.620
8	90.0	7.00	56.22	63.53	8.69	3085.1	2944.4	2523.3	2382.6	0.772	7.311
9	91.0	7.00	56.22	63.95	8.27	3077.2	2935.0	2524.9	2382.6	0.774	7.732
10	70.0	13.00	51.87	54.46	21.05	3318.8	3222.8	2489.6	2393.6	0.721	2.587
11	70.0	13.50	51.49	54.46	18.37	3230.3	3135.5	2489.4	2394.5	0.741	2.965
12	70.0	14.00	51.13	54.46	16.35	3162.9	3069.1	2489.2	2395.4	0.757	3.331
13	70.0	14.50	50.75	54.46	14.68	3106.3	3013.6	2489.0	2396.4	0.771	3.710
14	70.0	15.00	50.37	54.46	13.32	3059.3	2967.8	2488.9	2397.3	0.784	4.088
15	70.0	15.50	49.98	54.46	12.16	3018.5	2928.0	2488.7	2398.2	0.795	4.479

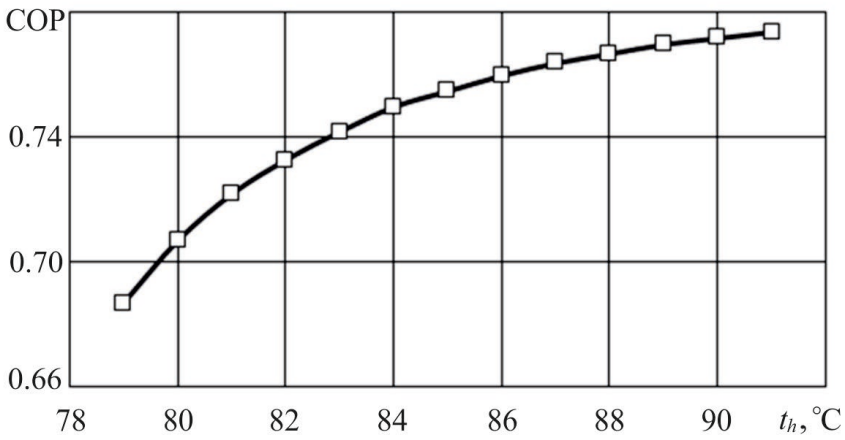

Figure 3 – Dependency of COP on temperature of heating medium at t_s = 7 °C

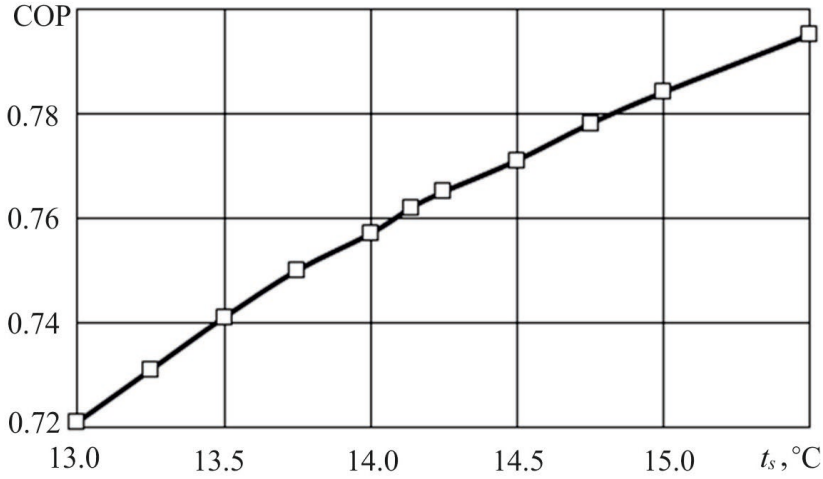

Figure 4 – Dependency of COP on temperature of cooled coolant at t_h = 70 °C

Thus, the results indicate that the operating range of final temperatures of the heating medium (from 80 °C to 84 °C) is significantly limited. It is impossible to utilize all the GE waste heat in one LBAC, while reducing its potential to 70 °C and cooling the coolant to 7 °C. The analysis also shows that the increase of final coolant temperature allows reducing the heating medium temperature (modes 10 – 15), and the solution degassing zone widens as well.

The scheme of simultaneous operation of two LBACs with the sequential movement of the heating and cooled media through them is suggested (Fig. 5) considering the character of change of parameters of the LBAC cycle. This is aimed at increasing the completeness of GE waste heat conversion and, accordingly, the completeness of cooling the coolant for air conditioning systems.

The heating medium first enters LBAC number 1 with a high-temperature generator and a low-temperature evaporator, and then flows to LBAC number 2 with a low-temperature generator and a high-temperature evaporator, as shown in Figure 5. The coolant is first cooled in the evaporator of LBAC number 2, and then the final cooling occurs in the evaporator of LBAC number 1.

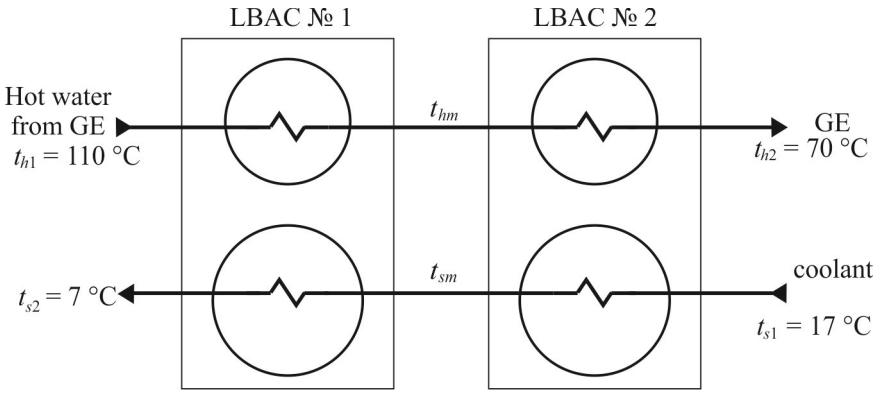

Figure 5 – Scheme of GE waste heat utilization using a system of two LBACs, where t_{hm} and t_{sm} are intermediate temperatures (after the first cooling stage) of heating medium and coolant, °C

A method of calculation of thermal modes of such a system is developed. The main calculation results are shown in Table. 2.

Table 2 – Calculation results of thermal modes of a system of two LBACs

t_{hm}, °C	t_{sm}, °C	ξ_{a1}, %	ξ_{r1}, %	ξ_{a2}, %	ξ_{r2}, %	$\Delta\xi_1$, %	$\Delta\xi_2$, %	b_{h1}	b_{s1}	η_1	η_2	η
79.0	14.54	56.2	58.7	50.7	54.5	2.53	3.73	0.775	0.754	0.687	0.772	0.707
80.0	14.34	56.2	59.2	50.9	54.5	2.98	3.59	0.750	0.734	0.707	0.767	0.722
81.0	14.14	56.2	59.7	51.0	54.5	3.43	3.44	0.725	0.714	0.722	0.762	0.733
82.0	13.94	56.2	60.1	51.2	54.5	3.87	3.28	0.700	0.694	0.733	0.755	0.740
83.0	13.73	56.2	60.5	51.3	54.5	4.31	3.14	0.675	0.673	0.742	0.749	0.745

Parameters shown in Table 2 are:

t_{hm} and t_{sm} are intermediate temperatures (after the first stage of cooling) of the heating medium and coolant, °C;

ξ_{a1}, ξ_{r1}, ξ_{a2}, ξ_{r2} are concentrations of weak and strong solutions of LiBr in LBAC number 1 and 2, respectively, %;

$\Delta\xi_1$ and $\Delta\xi_2$ are solution degassing zones in LBAC number 1 and 2, %;

η_1, η_2 and η are COP in LBAC number 1, 2 and in the entire system;

b_{h1} and b_{s1} are partial involvement of LBAC number 1 in lowering the temperature of heating and cooled media:

$$b_{h1} = \frac{t_{h1} - t_{hm}}{t_{h1} - t_{h2}}, \tag{24}$$

$$b_{s1} = \frac{t_{sm} - t_{s2}}{t_{s1} - t_{s2}}. \tag{25}$$

Analysis of the results shows that the degassing zone of LBAC number 1 widens, and the degassing zone of LBAC number 2 narrows during increase of the intermediate temperature of heating medium t_{hm}. Degassing zones of both machines become identical at t_{hm} = 81 °C and almost equal to the lower boundary (3.5 %) of the recommended range of values in the papers of other authors. LBAC number 1 utilizes 72.5 % of all available heat and provides a decrease of the waste coolant temperature by 71.4 % in this mode. COPs of LBAC number 1, 2 and the entire system are 0.722, 0.762 and 0.733, respectively.

The cooling capacity of GE JMS-620 is 2920 kW [1]. In this case, the cooling capacity generated by a system of two LBACs at COP of 0.733 is 2140 kW.

Conclusions. Dependencies of COP of heat into cold conversion and solution degassing zones on temperatures of heating and cooled media are established on a basis of mathematical modelling of thermal modes of a single-stage LBAC with a film generator, absorber and recirculation of solution of LiBr. A scheme of a system of two LBACs operating under different temperature modes is suggested. This allows fully utilizing GE JMS-620 waste heat, reducing its heat potential from 110 to 70 °C, and providing necessary temperature reduction of a coolant for an air conditioning systems from 17 to 7 °C. COP of heat into cold conversion of a system is 0.733. Research results evidence a potential of practical implementation of a suggested technical solution.

REFERENCES

1. Fedorov, S.D., Oblakevich, S.V., Radiuk, O.P. (2006). The problem of utilization coal mine methane in cogeneration plants and ways to solve it on the example of the mine name by A.F. Zasiadko. *Promelectro*, 5, 35-39

2. Semenenko, Ye.V., Diakun, I.L., Ruban, V.D. (2013). Prospects for the creation and implementation of energy complexes at coal mining enterprises. *ugol ukrainy*, 7, 30-34

3. Semenenko Ye.V., Diakun I.L. (2014) Economic prospects for coal methane utilization. In: *Prospects for the use of alternative and renewable energy sources in Ukraine*, **2**, 304-310

4. Voloshyn, O., Potapchuk, I., Yemelianenko, V., Zhovtonoha, M., Pertsevyi, V. (2019). Experimental study for the process of the borehole thermal reaming by means of the angular plasmatron. In: *E3S Web of Conferences, International Conference Essays of Mining Science and Practice*, **109** https://doi.org/10.1051/e3sconf/201910900113

5. Voloshyn, O.I., Potapchuk, I.Y., Zhevzhyk, O.V. (2018). Influence of the heat-transfer stream pressure on the surface of the rock in a process of the thermal reaming of the borehole. *Naukovyi Visnyk Natsionalnoho Hirnychoho Universytetu*, (2), 53-59 https://doi.org/10.29202/nvngu/2018-2/6

6. Kyrychenko, Y., Samusia, V., Kyrychenko, V., Romanyukov, A. (2013). Experimental investigation of aero-hydroelastic instability parameters of the deep-water hydrohoist pipeline. *Middle-East Journal of Scientific Research*, 18 (4), 530-534

7. Kyrychenko, E., Samusya, V., Kyrychenko, V., Antonenko, A. (2015). Thermodynamics of multiphase flows in relation to the calculation of deep-water hydraulic hoisting In: *New Developments in Mining Engineering*: *Theoretical and Practical Solutions of Mineral Resources Mining*, 305-311 https://doi.org/10.1201/b19901-54

8. Ilin, S.R., Samusya, V.I., Kolosov, D.L., Ilina, I.S., Ilina, S.S. (2018). Risk-forming dynamic processes in units of mine hoists of vertical shafts. *Naukovyi Visnyk Natsionalnoho Hirnychoho Universitetu*, (5), 64–71 https://doi.org/10.29202/nvngu/2018-5/10

9. Pivnyak, G., Samusia, V., Oksen, Y., Radiuk, M. (2014). Parameters optimization of heat pump units in mining enterprises. In: *Progressive technologies of coal, coalbed methane and ores mining*, 19-24 https://doi.org/10.1201/b17547-5

10. Oksen, Y., Samusia, O. (2014). Economic efficiency of heat pump technology for geothermal heat recovery from mine water. In: *Progressive technologies of coal, coalbed methane, and ores mining*, 191-194 https://doi.org/10.1201/b17547-35

11. Pivnyak, G., Samusia, V., Oksen, Y., Radiuk, M. (2015**)**. Efficiency increase of heat pump technology for waste heat recovery in coal mines. In: *New Developments in Mining Engineering*: *Theoretical and Practical Solutions of Mineral Resources Mining*, 1-4 https://doi.org/10.1201/b19901-2

12. Oksen, Y., Radiuk, M., Komissarov, Y., Kirsanov, M. (2019). Energy efficiency of cogeneration utilization of residual heat of flue gases during the drying of coal concentrate in pipe-dryers. In: *E3S Web of Conferences, International Conference Essays of Mining Science and Practice*, **109** https://doi.org/10.1051/e3sconf/201910900065

13. Oksen, Yu.I., and Radiuk, M.V. (2009). Investigation effectiveness of the use of waste heat gas piston installations for electricity generation, *Geotekhnicheskaya Mekhanika* [Geo-technical Mechanics], 81, 200-207

14. Oksen, Yu.I., Trofymova, E.P, Pisarev, V.P. (2019). Study of the efficiency of conversion of waste heat of gas reciprocating plants to electrical energy. *Hirnycha elektromekhanika ta avtomatyka*, 101, 104-109

15. Oksen, Yu.I., Trofymova, O., Bobryshov, O., Lukisha, A., Pryvalov, V. (2019). Gas engines waste heat recovery to electrical energy. In: *E3S Web of Conferences, International Conference Essays of Mining Science and Practice*, **109** https://doi.org/10.1051/e3sconf/201910900066

16. Barteczko, B., Nawrat, S., Rzepski, H., Schöler, J. (2001). Wytwarzanie w skojarzeniu prądu elektrycznego, ciepła i chłodu na potrzeby podziemnej klimatyzacji KWK "Pniówek". *Ciepłownictwo, Ogrzewnictwo, Wentylacja*, 32 (10), 22-27

17. Forrest S. Yount (2017) *Fundamentals Volume Subcommittee* (ASHRAE HANDBOOK COMMITTEE)

18. Baranenko, A.V., Tymofeevskyi, L.S., Dolotov, A.H., Popov, A.V. (2005). *Absorbtsionnyye preobrazovateli teploty*. Sankt-Peterburg: SPbGUNiPT

19. Galymova, L.V. (1997). *Absorbtsionnyye kholodilnyye mashiny i teplovyye nasosy*. Astrakhan: AGTU

20. Byikov, A.V. (1982). *Kholodilnyye mashiny: Spravochnik*. Moskva: Legkaya i pischevaya promyshlennost

21. Tseytlin, Yu.A., Abramova, T.G., Mogilevskiy, V.I., Roytman, V.F., Chernichenko, V.K. (1983). *Proyektirovaniye i ekspluatatsiya shakhtnykh sistem konditsionirovaniya vozdukha*. Moskva: Nedra

22. Tseitlin, Yu.A., Oksen, Yu.I., Roitman, V.F., Mogilevsky, V.I. (1985) Optimization of design of large refrigeration systems for deep mines. *Transactions of the Institution of Mining and Metallurgy (Section A: Mining industry*), 94, 217-218

23. Oksen, Yu.I., Semeshko, E.G. (1994) The effect of stochasticity of thermophysical properties and rock temperature on the distribution of cooling power of mine air coolers. *Fiziko-tekhnicheskiye problemy razrabotki poleznykh iskopayemykh*, 1, 87-91 https://doi.org/10.1007/BF02048779